# Isotope effects on L-H threshold and confinement in tokamak plasmas

CF Maggi[1], H Weisen[2], JC Hillesheim[1], A Chankin[3], E Delabie[4], L Horvath[5], F Auriemma[6], IS Carvalho[7], G Corrigan[1], J Flanagan[1], L Garzotti[1], D Keeling[1], D King[1], E Lerche[8], R Lorenzini[6], M Maslov[1], S Menmuir[1], S Saarelma[1], ACC Sips[9], ER Solano[10], E Belonohy[1], FJ Casson[1], C Challis[1], C Giroud[1], V Parail[1], C Silva[7] M Valisa[6] and JET Contributors*

*EUROfusion Consortium, JET, Culham Science Centre, Abingdon, OX14 3DB, UK*
*CCFE, Culham Science Centre, Abingdon OX14 3DB, UK*

[1]CCFE, Culham Science Centre, Abingdon, OX14 3DB, UK
[2]SPC, Ecole Polytechnique Federale de Lausanne, Switzerland
[3]Max-Planck Institut fuer Plasmaphysik, D-85748 Garching, Germany
[4]Oak Ridge National Laboratory, Oak Ridge, Tennessee, USA
[5]York Plasma Institute, Department of Physics, University of York, York YO10 5DD, UK
[6]Consorzio RFX, Corso Stati Uniti 4,35127 Padova, Italy
[7]Instituto de Plasma e Fusão Nuclear, Instituto Superior Tecnico, Lisboa, Portugal
[8]LPP-ERM/KMS, Association Eurofusion Belgian-State, TEC partner, Brussels, Belgium
[9]European Commission, Brussels, Belgium
[10]Laboratorio Nacional de Fusion, CIEMAT, Madrid, Spain

*****See the author list of "Overview of the JET results in support to ITER" by X. Litaudon et al., Nucl. Fusion **57** (2017) 102001, Special Issue on FEC 2016 Summaries and Overviews

**Abstract.** The dependence of plasma transport and confinement on the main hydrogenic ion isotope mass is of fundamental importance for understanding turbulent transport and, therefore, for accurate extrapolations of confinement from present tokamak experiments, which typically use a single hydrogen isotope, to burning plasmas such as ITER, which will operate in deuterium-tritium mixtures. Knowledge of the dependence of plasma properties and edge transport barrier formation on main ion species is critical in view of the initial, low-activation phase of ITER operations in hydrogen or helium and of its implications on the subsequent operation in deuterium-tritium. The favourable scaling of global energy confinement time with isotope mass, which has been observed in many tokamak experiments, remains largely unexplained theoretically. Moreover, the mass scaling observed in experiments varies depending on the plasma edge conditions. In preparation for upcoming deuterium-tritium experiments in the JET tokamak with the ITER-like Be/W Wall (JET-ILW), a thorough experimental investigation of isotope effects in hydrogen, deuterium and tritium plasmas is being carried out, in order to provide stringent tests of plasma energy, particle and momentum transport models. Recent hydrogen and deuterium isotope experiments in JET-ILW on L-H power threshold, L-mode and H-mode confinement are reviewed and discussed in the context of past and more recent isotope experiments in tokamak plasmas, highlighting common elements as well as contrasting observations that have been reported. The experimental findings are discussed in the context of fundamental aspects of plasma transport models.

## 1. Introduction

The dependence of energy and particle transport on the main ion isotope mass (A) is of fundamental interest for the understanding of turbulent transport and, therefore, for accurate predictions of confinement in burning devices. Future experiments, such as ITER, will

operate in deuterium-tritium mixtures, while current experiments typically use a single hydrogen isotope, usually deuterium. Knowledge of the dependence of plasma properties on isotope species is important for the initial, low-activation phase of ITER operations (hydrogen or helium).

For the analysis of transport processes in tokamak plasmas one can think of three main regions of the plasma volume, as shown schematically in Figure 1. In the very core of the plasma, physics processes are determined primarily by sawteeth (core MHD events) and by collisional (neoclassical [1]) transport. The core confinement region carries most of the plasma volume and therefore plays a key role for the overall confinement. In this region, turbulent transport – much higher than neoclassical – dominates and is thought to be due to small scale, ion Larmor radius size turbulence: $\rho \sim (A\ T)^{1/2} / B$, where T is the ion temperature and B the magnetic field. In this region, the local heat transport is predicted by quasi-linear models to follow the gyro-Bohm scaling: $\chi_{gB} \sim \rho^*$ (with $\rho^* = \rho/a$ the normalized ion Larmor radius, *a* the plasma minor radius and $\chi_{gB}$ the gyro-Bohm heat diffusivity), which results in an unfavourable dependence of local transport on isotope mass, $\chi_{gB} \sim A^{1/2}$. In H-modes, characterized by a region with steep pressure gradient at the plasma edge and improved energy and particle confinement above L-mode values, the gyro-Bohm scaling has been confirmed in numerous experiments in D plasmas, for the local electron transport see e.g. [2] and references therein. The local ion heat transport is also consistent with gyro-Bohm scaling in conditions when electron and ion heat diffusivities can be resolved, but departs from it depending on the variation of the fractional heat flux in the electron and ion heat channels [2].

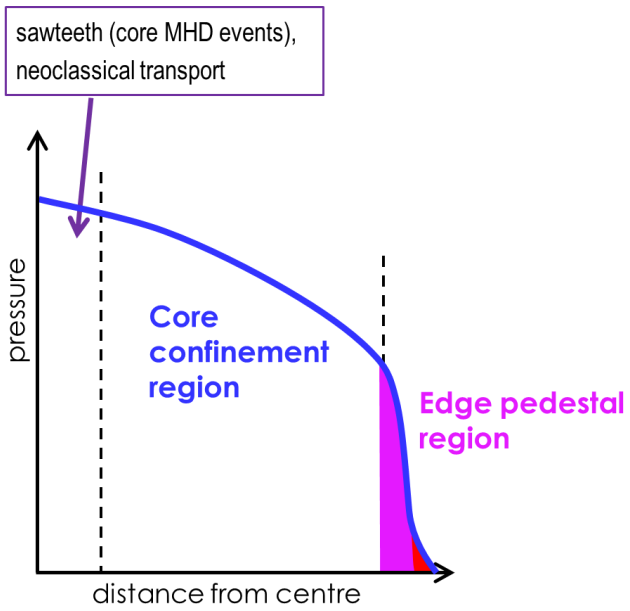


**Figure 1.** *Schematic representation of the radial pressure profile in a tokamak H-mode plasma, from plasma core to edge. The two vertical dashed lines indicate the three main regions of plasma confinement: the very core, governed by sawteeth and neoclassical transport; the core confinement region, with small scale ion turbulent transport; the edge pedestal region, with ELMs controlling the pedestal pressure height and reduced transport levels inter-ELM.*

In L-mode, tokamak experiments have shown in deuterium that the local transport follows the gyro-Bohm scaling for electrons and the Bohm scaling for ions, see e.g. [3], [4]: $\chi_i \sim \chi_B \sim T/eB$ (with $\chi_B$ the Bohm heat diffusivity). The Bohm scaling is therefore consistent with the absence of isotope dependence in the ion heat channel: $\tau_E \sim 1/\chi_B \sim A^0$.

The transition from low (L-mode) to high mode of confinement (H-mode) is characterized by a threshold in input power, $P_{L-H}$, whereby for input powers in excess of $P_{L-H}$ ion scale turbulence is strongly suppressed at the plasma edge, leading to the formation of an edge transport barrier (ETB) for both density and temperature in a region with large velocity shear, see e.g. [5], [6]. In the edge pedestal region, the transport is reduced to roughly neoclassical levels and periodic MHD events, the ELMs (Edge Localized Modes), limit the maximum pressure achievable at the top of the pedestal between subsequent ELM crashes. The pedestal region is strongly influenced by Scrape-off-Layer (SOL) physics: neutrals, radiation and impurity effects all have an impact on the pedestal. As the pedestal is influenced by SOL physics, also core and pedestal are strongly coupled in a wide range of H-modes, as observed in many tokamaks [7] and confirmed by modelling [8]: the pedestal pressure increases with the total plasma pressure as the core temperature gradients develop at constant gradient length, $L_T = \nabla T/T \cong$ constant. The pedestal, therefore, sets the boundary condition in H-modes. The ELMy H-mode is chosen as the primary mode of operation for ITER.

Over the years, several tokamak experiments and theoretical work have addressed the plasma transport properties with varying hydrogen isotope mass, primarily in hydrogen and deuterium plasmas, see e.g [9], [10], [11], [12], [13], [14], [15], [16], [17], [18], [19], [20], [21]. The TFTR tokamak [22] and the JET tokamak (JET DTE1) [23] are the only two tokamaks to have conducted experiments also in tritium and in the 50:50 deuterium-tritium mixtures required for burning plasmas. Different dependencies of the energy confinement, $\tau_E$, on isotope mass have been measured in L-mode and in H-mode [2]. The relationship between the local heat diffusivity and the global energy confinement is taken to be $\tau_E \sim a^2/\chi$. Although the strength of the isotope dependence often varies from tokamak to tokamak experiment, even in the same mode of confinement, all experiments consistently find a positive isotope dependence of confinement, $\tau_E \sim A^\alpha$, with $\alpha$ ranging from 0 to 0.85, which projects favourably to deuterium-tritium burning plasmas. On the other hand, the isotope effects observed experimentally are in contradiction of theoretical predictions of the gyro-Bohm scaling, from which one would expect an unfavourable dependence of $\tau_E$ on isotope mass with $\alpha = -0.5$. This discrepancy between theory and experiments still remains largely unexplained to date and presents a main challenge to the understanding of plasma turbulent transport. The main explanation put forward by theory regarding core heat transport has been linked to the effect of different isotopes on the shear flow and the resultant modification of the ion temperature gradient (ITG) driven turbulence [24]. Recently, gyrokinetic simulations with the GENE code have found a weak isotope effect in core heat transport in ITG/TEM (Trapped Electron Mode) regimes, but of smaller intensity than found in experiments [25]. Non-linear gyrokinetic simulations have shown that at high beta the core plasma micro-turbulence can depend on the isotope mass via multi-scale non-linear effects involving zonal flows, electromagnetic effects and *ExB* shear, which counteract the intrinsic, local, gyro-

Bohm scaling of plasma micro-turbulence [26]. The isotope effect on particle transport has been less studied. The recent work of [20] on the FT-2 tokamak reports an increase in particle confinement time by a factor of 1.4 from hydrogen to deuterium in comparable Ohmic plasmas, while no difference is observed in the energy confinement time [21], [20]. Global and local gyrokinetic simulations reproduce the isotope effect in particle transport [20]. However, gyrokinetic predictions for the total energy fluxes also indicate an isotope effect on energy transport, in contradiction of the ASTRA power balance analysis [20]. Nonetheless, in these plasmas geodesic acoustic modes (GAM) are found with larger amplitude in deuterium than in hydrogen both in experiment and in simulations, as well as a high correlation between turbulent transport bursts and GAM [21], suggesting the need to account for zonal flows in the analysis of the energy fluxes [20].

As the JET tokamak prepares for new deuterium-tritium experiments in 2019/20, with improved edge, neutrons and fast particles diagnostics, as well as with the ITER-like Wall (W in the divertor and mainly Be in the main chamber), a thorough experimental investigation of isotope effects in hydrogen, deuterium and tritium plasmas is being carried out, in order to provide stringent tests to plasma energy and particle transport models. Experiments in deuterium, hydrogen and hydrogen-deuterium mixtures were carried out in 2016. Between 2018 and 2019 a series of campaigns will cover studies in deuterium and tritium plasmas, followed by a second campaign in hydrogen and hydrogen-tritium and hydrogen-deuterium mixtures. A final campaign in deuterium is then foreseen, to complete the scenario optimization before the deuterium-tritium phase.

In the next three sections of the paper the isotope effects on L-mode (Section 2), L-H threshold (Sections 3) and H-mode (Section 4) are briefly reviewed and recent findings of isotope effects in tokamak plasmas are presented and discussed. A summary and conclusions are drawn in Section 5.

## 2. L-mode

Over the past two decades several tokamak experiments have confirmed that in L-mode the local energy transport follows the short-wavelength gyro-Bohm scaling for electrons, $\chi_e \sim \chi_{gB}$, see e.g. [3], while the ions follow the long-wavelength Bohm scaling, $\chi_i \sim \chi_B$, see e.g the review of [2] and references therein. As the Bohm scaling is independent of isotope mass, $\tau_E \sim 1/\chi_B \sim A^0$ would be predicted for the ion energy transport, namely consistent with no isotope dependence. On the other hand, regression of multi-tokamak data for the L-mode thermal energy confinement time has yielded the ITER97-L scaling [27], $\tau_{E,th}$ (ITER97-L) = $0.023\ I_P^{0.96}\ B_T^{0.03}\ P_{abs}^{-0.73}\ n_e^{0.40}\ A^{0.2}$ (with $I_P$ the plasma current [MA], $B_T$ the toroidal magnetic field [T], $P_{abs}$ the absorbed input power [MW] and $n_e$ the central line averaged density [$10^{19}$ $m^{-3}$]), which exhibits a positive isotope mass dependence, in contradiction of both gyro-Bohm and Bohm scaling.

Recent L-mode experiments in ASDEX Upgrade (AUG) with electron cyclotron resonance heating (ECRH) have compared two L-mode discharges in hydrogen and in deuterium, where the normalized ion gyroradius $\rho^*$ differed by $\sqrt{2}$, which is the square root of the mass ratio, while other dimensionless parameters were kept constant [18]. $\tau_{E,th}$ (H) =

83 ms was lower than $\tau_{E,th}$ (D) = 110 ms. Power balance and perturbative transport analyses revealed that the electron heat transport was unaffected by the change in isotope mass. Due to the central electron heating scheme used, $T_e > T_i$ in the plasma core, thus allowing for measurement of the electron-ion collisional exchange term in the energy balance equation with sufficient accuracy: $P_{e-i} \sim n^2 (T_e - T_i)/(A\ T_e^{3/2})$. Due to the mass dependence of $P_{e-i}$, $P_{e-i}(H) = 2 \times P_{e-i}(D)$ and it is found that the additional ECRH heating required in hydrogen to match the profiles in deuterium is transported by the ion channel and $Q_i(H) > Q_i(D)$, as shown in Figure 2 [18]. The uncertainties in the measured ion temperature gradients are too large to distinguish between hydrogen and deuterium in the power balance transport analysis and $\chi_i^{PB}$ = 1-3 $m^2/s$ are reported for both ion species. The reduced $\tau_{E,th}$ in hydrogen in these low β plasmas (where β is the ratio of the plasma kinetic pressure to the magnetic pressure) is explained by the mass dependence in the collisional energy exchange between electrons and ions and not by a gyroradius effect. It is also noted in [18] that an increase in ion heat transport due to isotope mass effects is not expected for such ITG turbulence dominated plasmas. This result was also confirmed with ASTRA simulations, which show that the experimental profiles and global energy confinement can be reproduced when using the same coefficients for hydrogen and deuterium in the transport code [18].

This same mechanism is found to explain the weak, but positive isotope effect on thermal energy confinement observed from hydrogen to deuterium Ohmic discharges in JET-ILW, where $T_i < T_e$ is measured in the plasma core, although in this case an isotope effect on the ion heat transport is not excluded by the data [28].

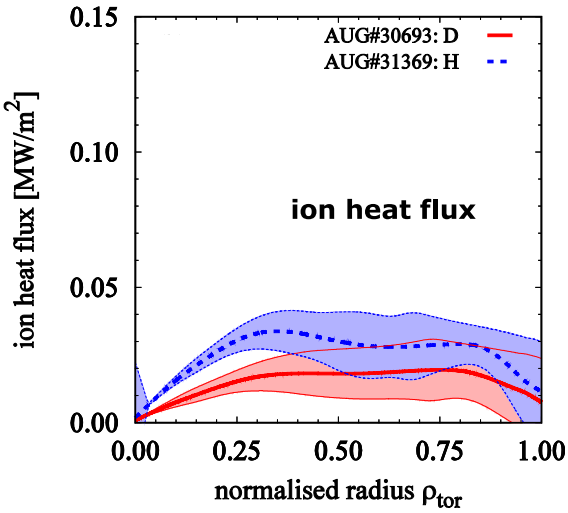


***Figure 2.*** *Radial profile of ion heat flux for deuterium (red) and hydrogen (blue) ECRH heated L-modes in AUG (reprinted from [18]).*

The mass dependence of the collisional ion-electron heat exchange cannot, however, be invoked to explain the lower $\tau_{E,th}$ in hydrogen than in deuterium when $T_i \cong T_e$, that is when the ion-electron heat exchange term cannot be quantified within experimental uncertainties. This is the case of L-mode plasmas obtained in recent JET-ILW experiments with neutral beam (NBI) heating at 2.5MA/3.0T. The NBI power was scanned from 1 MW to 9 MW in both hydrogen and deuterium while keeping the plasma density constant to $n_e \sim 3.0 \times 10^{19}\ m^{-3}$

(obtained with feedback control on the injected gas). The accuracy in the NBI power calibration is estimated to be of order 10%, with the largest errors originating from the beam neutralisation and beam transmission measurements (obtained by a combination of test bed measurements and simulations). The transmission in H is lower (70%) than that in D (75%) and it's accounted for in the calibration factor. Based on the available data, the relative accuracy of the NBI power calibration is believed to be the same for hydrogen and deuterium beams. We note that at all NB power levels in the scan the ratio of electron to ion NB heating was the same in hydrogen and in deuterium, as shown in Figure 3, due to H-NBI operation at lower NB voltage (60 – 70 kV) than with D-NBI (80 – 90 kV). The calculations of Figure 3 were carried out with the PENCIL neutral beam deposition code [29].

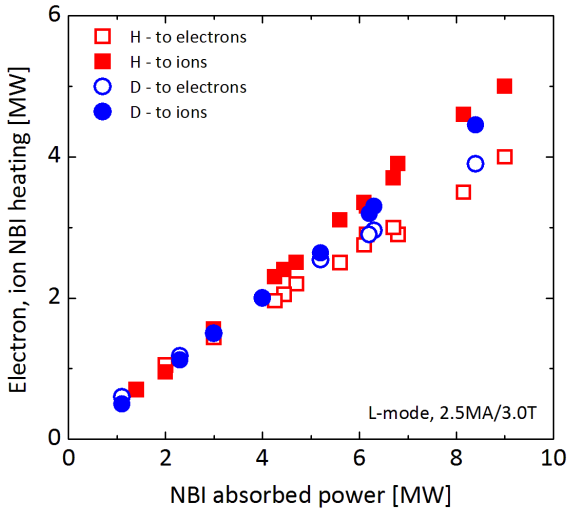


***Figure 3****. Total neutral beam electron heating (open symbols) and ion heating (solid symbols) versus total NB absorbed power for the hydrogen (red squares) and deuterium (blue circles) L-mode power scans at 2.5MA/3.0T at constant density in JET-ILW.*

In the experiments, a larger gas puff rate and NBI fuelling were needed in hydrogen to achieve the same density as in deuterium, indicating worse particle confinement in hydrogen. Higher NBI power was required in hydrogen to achieve the same total stored energy as in deuterium. After subtraction of the fast ion energy contribution from the stored energy inferred by the MHD equilibrium reconstruction EFIT, the thermal stored energy is still found to be lower in hydrogen than in deuterium and regression of the measured $\tau_{E,th}$ data gives: $\tau_{E,th} \sim A^{0.15\pm0.02} P_{abs}^{-0.63\pm0.02}$, as shown in Figure 4, in broad agreement with the favourable mass dependence of the ITER97-L scaling. The thermal stored energy calculation described above is in agreement, within 10%, with that obtained by the TRANSP code [30] with input the measured kinetic profiles integrated over the plasma volume. The positive isotope dependence of $\tau_{E,th}$ observed in JET-ILW L-modes is in contradiction of both gyro-Bohm and Bohm scaling.

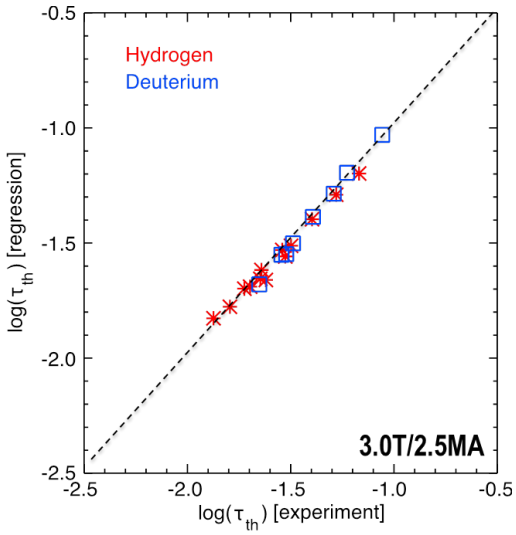


***Figure 4.*** *Log-log regression of the measured L-mode thermal energy confinement time in JET-ILW for hydrogen (red asterisks) and deuterium (blue squares) plasmas at 2.5MA/3.0T at constant plasma density with respect to isotope mass and absorbed power:* $\tau_{E,th} \sim A^{0.15\pm0.02} P_{abs}^{-0.63\pm0.02}$.

The JET-ILW plasmas of this dataset are of relatively high collisionality, leading to strong coupling of ions and electrons. A simple equipartition analysis shows that if $T_i$ were to exceed $T_e$ by 20%, the net power to the ions would be negative over a significant portion of the radial profile in over half of the cases analysed. The core $T_i$ profile data have large systematic uncertainties (of order 20% overall). They were measured either by Ne X, n = 11-10, charge exchange recombination spectroscopy (CXRS), using diagnostic Ne puffs, and/or by bulk ion CXRS. Within the uncertainties of the available data, $T_i \cong T_e$, but potential, small differences between core ion and electron temperatures cannot be resolved. Conversely, the edge $T_i$ profiles are measured by CVI, n = 8-7, CXRS and have higher accuracy. At the plasma edge $T_i = T_e$, consistently through the L-mode dataset. Under these conditions, both in hydrogen and in deuterium plasmas for the transport analysis we have assumed $T_i \cong T_e$ within experimental uncertainties of the $T_i$ profile data and the transport analysis has been carried out based on the electron kinetic profiles. The sawtooth inversion radius is at $\rho_{tor}$ = 0.22 – 0.26 (corresponding to $\rho_{pol}$ = 0.3 – 0.35), depending on the individual discharge, where $q_\psi$ ~1. In the transport region, the inverse normalized temperature gradient length is measured for electrons, $R/L_{Te} \cong R/L_{Ti}$, as shown in Figure 5. Therefore, under these conditions, the electrons and/or ions are stiff. An error analysis, with the above uncertainties, shows that a meaningful species-resolved transport analysis is unfortunately not possible. Only the one-fluid, effective heat diffusivity, $\chi_{eff}$, can be extracted and Figure ~~4~~5 shows that at mid-radius ($\rho_{tor}$ = 0.5) hydrogen and deuterium plasmas have comparable $\chi_{eff}$ at all input power levels of the L-mode power scan, in contradiction of the unfavourable gyro-Bohm dependence predicted by theory, $\chi_{gB} \sim A^{1/2}$.

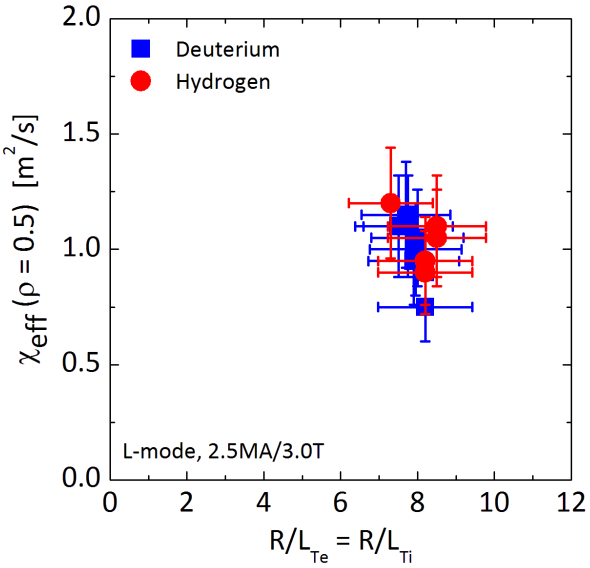


***Figure 5.*** *One-fluid effective heat diffusivity, $\chi_{eff}$, vs $R/L_{Te} \cong R/L_{Ti}$ at $\rho_{tor}$ = 0.5 for the L-mode power scans in hydrogen and deuterium at constant density, at 2.5MA/3.0T in JET-ILW: hydrogen (red circles) and deuterium (blue squares).*

While no significant isotope effect is found in the L-mode core heat transport under these conditions, a strong, favourable isotope effect is found both in particle and heat transport at the plasma edge from detailed EDGE2D/EIRENE [31], [32] interpretative simulations. Two representative discharges of the 2.5MA/3.0T power scans were analysed, in the phase marked by the black, dashed rectangle in Figure 6, where higher NBI power was required in hydrogen to achieve the same total stored energy as in deuterium and larger gas puff rate and NBI fuelling were required in hydrogen to achieve the same central line averaged density as in deuterium. The corresponding electron kinetic profiles, in the steady time window analysed, are shown in Figure 7, where $n_e$ is measured by reflectometry and $T_e$ by the Electron Cyclotron Emission diagnostic (ECE). The $n_e$ and $T_e$ profiles measured by High Resolution Thomson Scattering (HRTS) are in very good agreement with those by reflectometry and ECE, respectively (not shown in Figure 7 for simplicity).

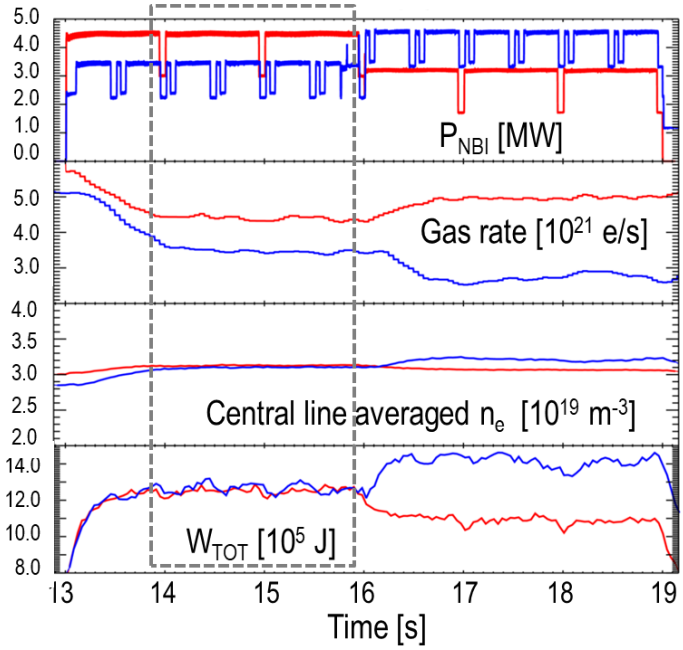


***Figure 6.*** *Time traces of main plasma parameters for two L-mode discharges in JET-ILW at 2.5MA/3.0T in hydrogen (red, #91450) and deuterium (blue, #89723). From top to bottom: NBI input power, injected gas rate, central line averaged density and total stored energy. The dashed black rectangle indicates the time window where the H and D discharges achieve the same density and same total stored energy, obtained by larger NBI heating and larger gas puffing rate in the hydrogen pulse.*

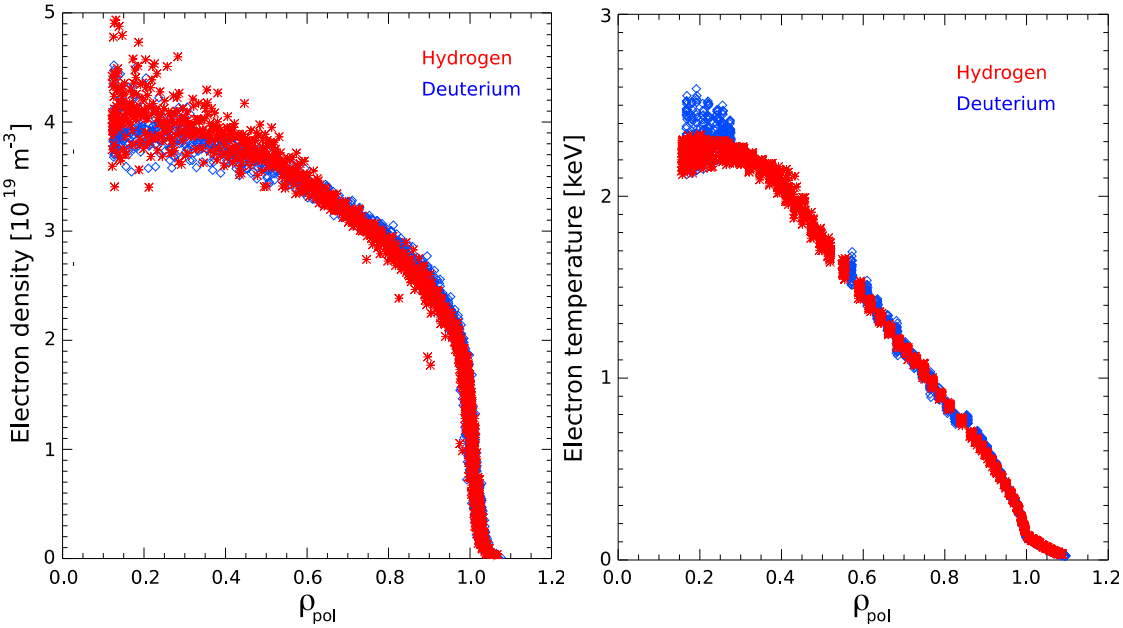


***Figure 7.*** *Composite profiles of electron density (measured by reflectometry) and temperature (measured by ECE) for the L-mode discharges of Figure 6: hydrogen (red) pulse #91450 and deuterium (blue) pulse #89723, for the steady time window between 14.0 – 16.0 s, where $P_{NBI}(H)$ = 4.5 MW and $P_{NBI}(D)$ = 3.4 MW and injected gas rates $\Gamma(D) = 3.5 \times 10^{21}$ e/s and $\Gamma(H) = 4.4 \times 10^{21}$ e/s.*

The edge anomalous transport coefficient of electron particle diffusion, $D_{perp}$ ($\Gamma_e = - D_{perp} \nabla n_e$), and of ion & electron heat diffusivity, $\chi_{e,i}$ ($q_{e,i} = - n_{e,i} \chi_{e,i} \nabla T_{e,i}$) were obtained by fitting the EDGE2D/EIRENE solutions to the experimental upstream profiles. The latter were measured by profile reflectometry and HRTS for $n_e$ and by HRTS for $T_e$ (as the ECE diagnostic does not have sufficient spatial resolution near the LCFS). The edge experimental profiles and the EDGE2D/EIRENE profiles fitted to the experimental data (black lines) are shown in Figure 8 for the two hydrogen and deuterium discharges of Figure 6. The experimental data are averaged in the steady time window (14.0 – 16.0 s). While the edge $T_e$ profile is more uncertain, in particular for the H shot, the $n_e$ profile data from reflectometry have high accuracy and allow for a clear distinction in H and D edge particle diffusion coefficients. Figure 9 shows that larger transport coefficients D and $\chi_{e,i}$ are required in hydrogen than in deuterium - both inside and outside the Last Closed Flux Surface (LCFS) – to fit the modelled $n_e$ and $T_e$ profiles to the experimental data. In particular, the good spatial resolution of the edge $n_e$ profile measured with reflectometry allows for the computation of a radial structure in $D_{perp}$.

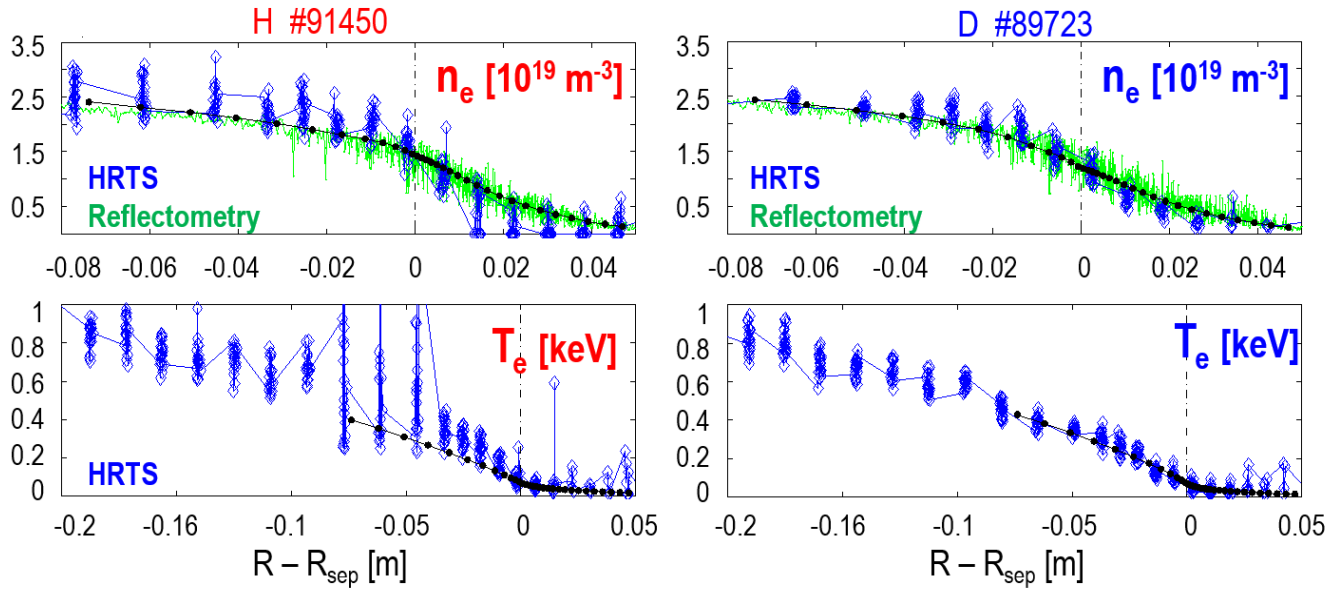


***Figure 8.*** *Radial profiles of $n_e$ and $T_e$ for the hydrogen (left, #91450) and deuterium (right, #89723) L-mode discharges of Figure 6, time averaged between 14.0 and 16.0 s, that is the phase at same total stored energy and plasma density (larger NBI power and gas puffing in hydrogen than in deuterium as indicated by the dashed black rectangle in Figure 6). HRTS data are in blue, profile reflectometry data are in green and EDGE2D/EIRENE fits to the experimental profiles are in black. $R_{sep}$ is the major radius at the magnetic separatrix projected at the outer midplane. $n_{e,sep}$ = 1.4 x $10^{19}$ m-3 / $T_{e,sep}$ = 70 eV for hydrogen and $n_{e,sep}$ = 1.2 x $10^{19}$ $m^{-3}$ / $T_{e,sep}$ = 70 eV for deuterium.*

An additional aspect of the 2D modelling is that for a given neutral source it is not possible to fit the experimental density profiles by only adjusting $D_{perp}$. Values of albedo at the cryopump surfaces (in the divertor corners of the EDGE2D grid) also require adjustment.

In particular, the solutions shown in Figure 8 and 9 were obtained with albedo @ pump = 0.925 for the hydrogen case and albedo @ pump = 0.91 for the deuterium case. In EDGE2D/EIRENE the pumping albedo is defined to be equal to [1 – sticking probability of $H_2$ (or $D_2$) gas to the cryosurface]. The sticking probabilities were shown to be higher for deuterium than for hydrogen from neutral beam test bed results [33], which implies lower albedo values for deuterium than for hydrogen, in qualitative agreement with the EDGE2D/EIRENE simulations.

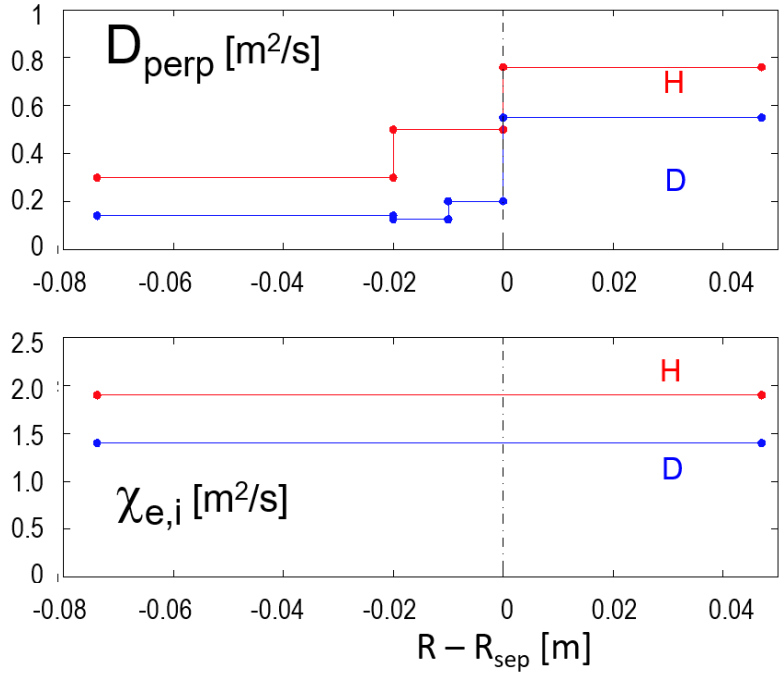


***Figure 9.*** *Radial profiles of perpendicular particle diffusivity (top) and electron & ion heat diffusivity (bottom) coefficients for hydrogen (red) and deuterium (blue) derived from interpretative EDGE2D/EIRENE simulations of the L-mode discharges of Figure 6, in the phase at same total stored energy and plasma density (and larger NBI power and gas puffing in hydrogen than in deuterium), as indicated by the dashed black rectangle in Figure 6.*

Consistent with the larger edge particle transport in hydrogen than in deuterium, larger edge density fluctuations (relative to their value in the Ohmic phase of the deuterium discharge) were measured with Doppler reflectometry [34] in hydrogen than in deuterium for the same $P_{NBI}$. The probed wavenumbers for the pulses in this paper are in the range 3-4 $cm^{-1}$. Figure 10 illustrates the case of two discharges in hydrogen and deuterium with $P_{NBI}$ = 3 MW, although this result was obtained at all power levels in the L-mode dataset.

In summary, recent experiments in the L-mode regime in hydrogen and deuterium plasmas show that in conditions where $T_i$ and $T_e$ are decoupled in the plasma core, such as ECRH heated plasmas in AUG or Ohmic plasmas in JET-ILW, the lower thermal energy confinement time measured in hydrogen can be explained by the isotope mass dependence of the i-e heat exchange term in the energy balance equation. On the other hand, this mechanism cannot be invoked with certainty to explain the favourable isotope effect on $\tau_{E,th}$ in JET-ILW L-modes with NBI heating, where $T_i$ and $T_e$ are strongly coupled and therefore the e-i heat

exchange term cannot be measured outside experimental error bars. In these plasmas a negligible isotope effect is found in the plasma core from transport analysis setting $T_i = T_e$ (within experimental error bars of the Ti data), while a strong, positive isotope effect is found at the plasma edge, both inside and outside the LCFS, on both energy and particle transport. The combination of negligible core and strong edge isotope effects yield the weak, but favourable isotope dependence on $\tau_{E,th} \sim A^{0.15}$ measured in JET-ILW L-modes, in broad agreement with the isotope mass dependence of the multi-tokamak ITER-97L scaling ($A^{0.2}$).

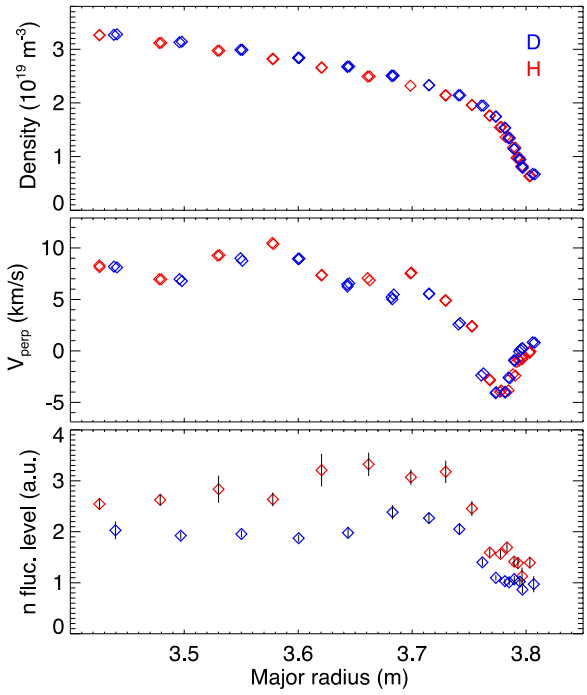


***Figure 10.*** *From top to bottom, radial profiles of: edge density (measured with profile reflectometry), $v_{perp}$ and density fluctuation levels, measured with DBS, in JET-ILW in two L-mode discharges in hydrogen (red, #91450, 17.0 – 18.0 s) and deuterium (blue, #89723, 14.0 – 15.0 s) at 2.5MA/3.0T, $P_{NBI}$ = 3 MW. The density fluctuation levels are relative to those measured in the Ohmic phase of the deuterium discharge. The LCFS is at 3.79 (± 0.01) m.*

## 3. L-H threshold

Despite much progress in theoretical work and a growing body of detailed experimental measurements on L-H transition dynamics in many tokamaks, a first principles physics model of the L-H transition with predictive capability is still missing. Extrapolations to future experiments therefore still rely on empirical scalings, such as the 2008 ITPA scaling: $P_{L\text{-}H,08} \sim n_e^{0.717}\, B_T^{0.803}\, S^{0.941}$ [35], with $n_e$ [$10^{20}$ m$^{-3}$] the line averaged density, $B_T$ [T] the toroidal magnetic field and S [m$^2$] the plasma surface area. This scaling carries at least a factor of two uncertainty, due to additional dependencies of $P_{L\text{-}H}$ not included in the scaling.

It has been known for several decades that the H-mode power threshold has a favourable dependence on isotope mass: $P_{L\text{-}H} \sim 1/A$, as measured in many tokamak experiments in hydrogen and deuterium plasmas, see e.g. [9], [36], [37], [38] as well as in hydrogen,

deuterium, tritium and deuterium-tritium in JET [39]. These observations typically pertain to the high density branch of $P_{L-H,}$ namely where $P_{L-H}$ increases with density. This result projects to H-mode access in a fusion reactor with 50:50 deuterium-tritium mixture with about 20% less power than in a deuterium plasma.

Recent isotope experiments on the L-H threshold in JET-ILW in hydrogen and deuterium plasmas, with ICRH heating, have highlighted a stronger isotope dependence of $P_{L-H}$ in the low density branch [40], of order a factor of three, as shown in Figure 11, which may be indicative of edge L-mode turbulence of different nature in the low and high density branch [41], [34]. The JET-ILW measurements differ from results reported from AUG, where the ~ 1/A isotope dependence of $P_{L-H}$ was observed both in the low and in the high density branch [38]. The difference in H-mode threshold between hydrogen and deuterium plasmas in JET-ILW is much larger for NBI-heated plasmas, reaching up to a factor of 4. It is currently being investigated whether this is due to an effect of NB torque on $P_{L-H}$, as observed on DIII-D [37], or to the partition between ion and electron energy fluxes at the L-H transition, as proposed in [42].

L-H transitions in 50:50 hydrogen-deuterium mixtures in JET-ILW resulted in $P_{L-H}$ values intermediate between the pure hydrogen and deuterium cases, which had isotope purity > 98-99%, as measured by Balmer-$\alpha$ spectroscopy at the plasma edge. The largest variation in $P_{L-H}$ when varying the isotope ratio is observed at high and low H/(H+D) ratios, while little variation is found for $0.2 < H/(H+D) < 0.8$ [40]. This was an unexpected result and remains as yet unexplained. The strong variation in $P_{L-H}$ at small levels of hydrogen in deuterium and of deuterium in hydrogen plasmas may indicate a role of ion-ion collisions, where the product of the hydrogenic isotope densities gives a parabolic dependence for the collision rate [40]. An important implication of this finding is that it's imperative to achieve the highest isotope purity (> 98%) in experiments when studying hydrogen vs deuterium plasmas, in order to prevent spurious conclusions from the experimental observations.

A similar, non-linear dependence on isotope mixtures is observed for H-mode energy confinement: the thermal stored energy, $W_{th}$, is lower in hydrogen than in deuterium (see Section 4) and the largest variations in $W_{th}$ between the two species is observed for $0 < H/(H+D) < 0.1$ and $0.9 < H/(H+D) < 1.0$ [43].

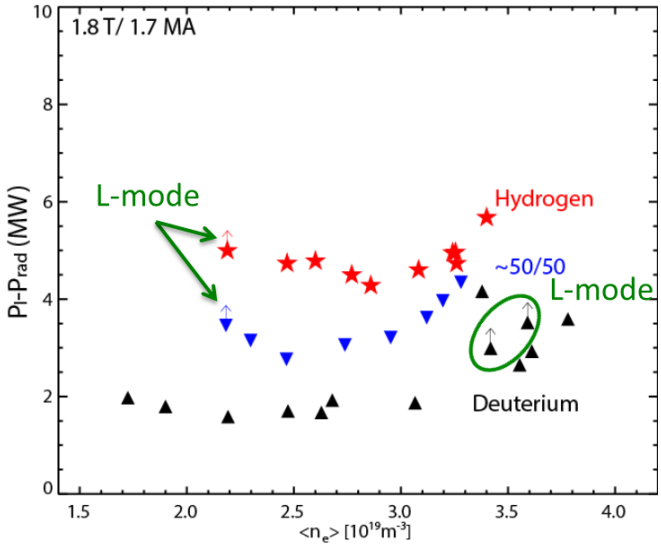


***Figure 11.*** *L-H transition power threshold in JET-ILW hydrogen (red stars), deuterium (black up-triangles) and 50:50 H-D mixture (blue down-triangles), with ICRH heating only at 1.8T/1.7MA.*

The isotope dependence of $P_{L-H}$ remains as yet unexplained. Here we put forward the hypothesis, based on the JET-ILW observations, that, at least in the high density branch, the favourable isotope effect on $P_{L-H}$ is a consequence of the favourable isotope effect on transport at the L-mode edge. As discussed in Section 2, a positive isotope effect is found in L-mode at the plasma edge, both for particle and heat transport and the ETB forms in the plasma region where the isotope effect is found in L-mode. In the high density branch, at the L-H transition, the same edge kinetic profiles ($n_e$, $T_e$) are measured in hydrogen and deuterium when $P_{loss}(H) \sim 2 \times P_{loss}(D)$ [41], as shown in Figure 12. As evidenced by a large body of experimental and theoretical work, the L-H transition is triggered when the $E_r$xB shearing rate is of order of the growth rate of the L-mode edge turbulence, $\gamma_E = \nabla E_r / B \sim \gamma_{turb}$. In addition, considering that $E_r = \nabla p_i/(Z\ e\ n_i) - v_i$xB does not depend on isotope mass (except for mass effects in the coefficients for the neoclassical poloidal rotation), then the larger $P_{L-H}$ measured in hydrogen than in deuterium may only be a consequence of the larger input power required to suppress the higher levels of L-mode edge turbulence in hydrogen, via the dominant diamagnetic shear, and not of an isotope effect on the L-H transition per se.

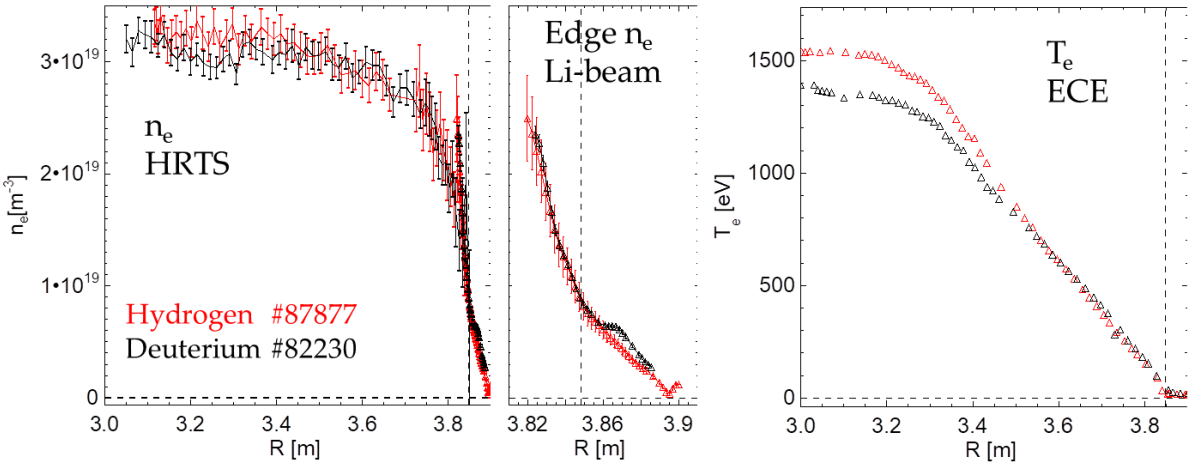


***Figure 12.*** *Comparison between hydrogen (red) and deuterium (black) $n_e$ and $T_e$ radial profiles in L-mode just before the L-H transition in JET-ILW. The vertical, dashed lines in the three panels indicate the position of the LCFS. $T_i$ (as measured by edge CXRS) = $T_e$ in the edge region (reproduced from ref. [41]).*

## 4. H-mode

Isotope experiments in JET with the C wall (JET-C) in hydrogen, deuterium, tritium and deuterium-tritium showed for ELMy H-modes no isotope dependence of thermal energy confinement time $\tau_{E,th} \sim A^{0.03\pm0.1}$, due to strong, positive isotope dependence at the pedestal, $W_{ped} = 0.45\ B^{1.2}\ (A/2)^{0.96}$ and weak, negative isotope dependence in the plasma core, $\tau_{th,core} \sim A^{-0.16\pm0.1}$ [14] (the latter is in approximate agreement with the gyro-Bohm dependence, $\tau_{gB} \sim A^{-0.5}$). The strong isotope dependence at the pedestal was also supported by ELM losses measurements: in the type I ELMy H-mode regime larger ELMs were observed in tritium than in deuterium in discharges at 2.7T/2.6MA at the same input power of ~ 10 MW of NBI heating [44], while hydrogen discharges did not have type I ELMs due to the limited H-NBI power (and larger H-mode threshold). These experiments were, however, hampered by diagnostic resolution at the plasma edge.

A rather different picture, on the other hand, has been put forward by hydrogen and deuterium isotope studies in JT-60U, where, as in other tokamaks, $\tau_{E,th}$ is found to increase with isotope mass, but, unlike in JET-C, it is concluded that the favourable isotope effect stems from the plasma core, with no direct isotope effect in the pedestal region [17], [16], [15]. Comparative hydrogen and deuterium type I ELMy H-modes were obtained with matching thermal stored energy, $W_{th}$, by raising $P_{NBI}$ in hydrogen to match the electron and ion temperature profiles, while the $n_e$ profile was automatically matched in the two species and the toroidal rotation profile was similar, although co-current in deuterium and ctr-current in hydrogen, as shown in Figure 13. It is thus likely that the radial electric field would be somewhat different in the two cases. The effective ion charge $Z_{eff}$ increased for deuterium up to 2.4 at the maximum input power, while it remained approximately constant with power at $Z_{eff} = 1.5$ in hydrogen. The two H-modes in hydrogen and deuterium at same $W_{th}$ had similar $Z_{eff} \sim 1.5$ [17]. The larger ion heat flux, $Q_i$, in hydrogen, at same $W_{th}$, resulted in larger $\chi_i$ in hydrogen than in deuterium over the entire plasma minor radius [17], see Figure 13. The

same pedestal structure was measured in the edge $T_i$ profile in hydrogen and deuterium (same pedestal height, width and gradient) at matched normalized pressure $\beta_{pol}$ in the two ion species [15], but differing $\rho^*_{pol}$, which led to the conclusion that no direct isotope effect is observed in the pedestal region in JT-60U. The poloidal beta is defined as $\beta_{pol} = p / (<Bp>^2 / 2\mu_0)$, with $p$ the plasma kinetic pressure and $<B_p>$ the average poloidal magnetic field. It is however always the case that when hydrogen and deuterium ELMy H-modes are compared at the same $I_P/B_T$ and same input power a larger pedestal pressure is observed in deuterium than in hydrogen [17]. This is explained by: i) the measurement of a positive isotope effect of core ion heat transport [16], [17], whereby profile stiffness is observed in both hydrogen and deuterium H-modes, but with a smaller $L_{Ti}$ for the heavier isotope mass, see Figure 14; ii) the pedestal pressure increasing with total $\beta_{pol}$ in both hydrogen and deuterium; iii) deuterium plasmas achieving larger $\beta_{pol}$, due to reduction in core ion heat transport compared to hydrogen (see (i)) and larger fast ion energy, as the fast ion slowing down time, $\tau_S$, increases with isotope mass: $\tau_S \sim A^{1/2} T^{3/2}$ ; iv) extension of the pedestal stability boundary with larger $\beta_{pol}$ for deuterium than for hydrogen [17].

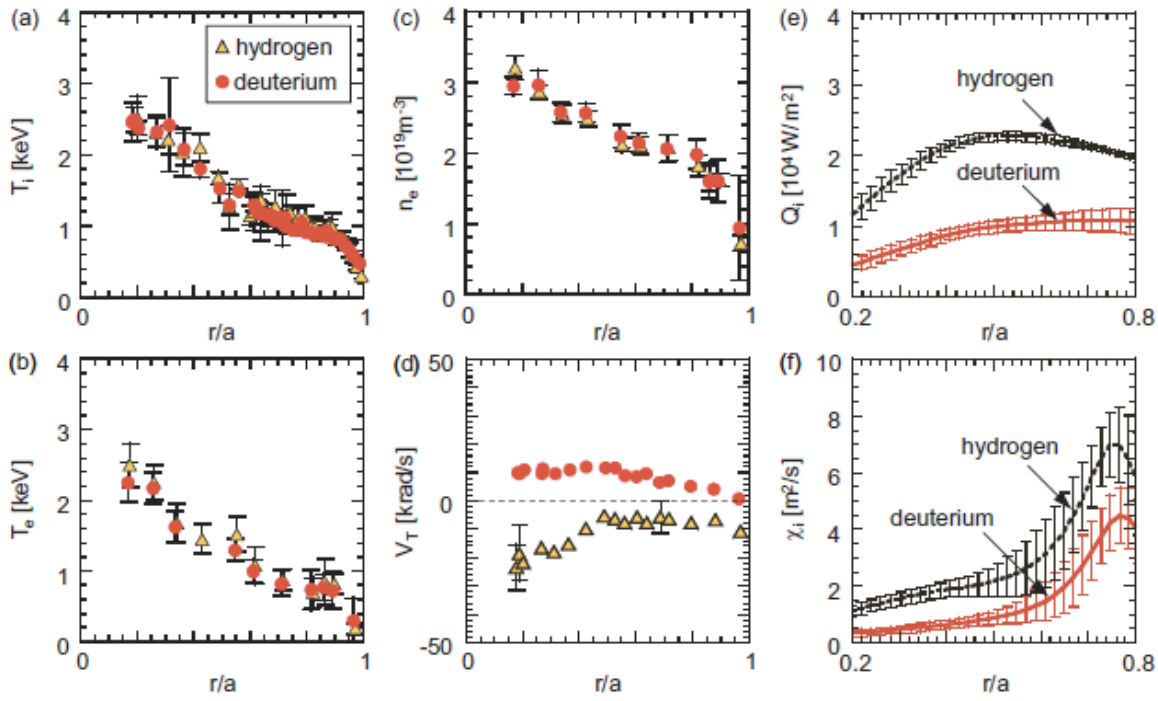


***Figure 13.*** *Radial profiles of (a) ion temperature $T_i$, (b) electron temperature $T_e$, (c) electron density $n_e$, (d) toroidal velocity $v_T$, (e) ion conductive heat flux $Q_i$ and (f) ion heat diffusivity $\chi_i$ for hydrogen (yellow triangles) and deuterium (red circles) H-modes with the same $W_{th}$ in JT-60U (reprinted from [17]).*

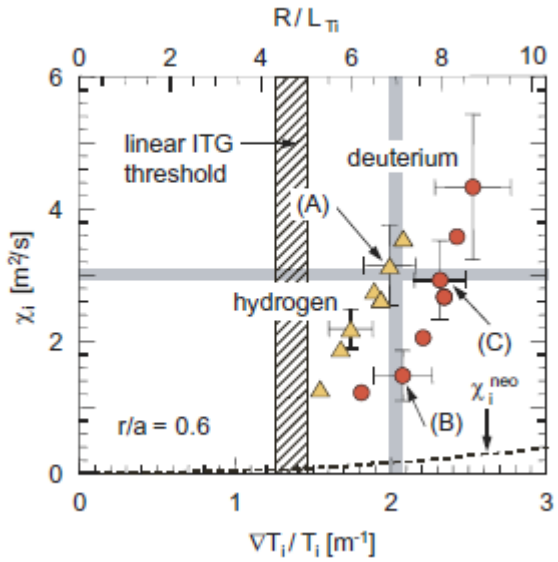


***Figure 14.*** *Ion heat diffusivity $\chi_i$ vs $\nabla T_i$ or $R/L_{Ti}$ at r/a = 0.6 for power scans in hydrogen and deuterium H-mode plasmas in JT-60U (reprinted from [17]).*

In recent isotope experiments in JET-ILW in hydrogen and deuterium plasmas, Type I ELMy H-modes could be obtained in hydrogen, both at 1MA/1T and at 1.4MA/1.7T. At 1MA/1T, H-mode discharges were obtained with H-NBI and D-NBI heating only, respectively. We note that the maximum power delivered by H-NBI was 10 MW in these experiments. Therefore, for the 1.4MA/1.7T dataset the discharges had NBI heating only in the deuterium plasmas and either H-NBI only (up to 10 MW) or a combination of 9-10 MW H-NBI and 2.5-5.5 MW ICRH (51 MHz, H majority, 2$^{nd}$ harmonic) heating in the hydrogen plasmas in order to maximize the available auxiliary heating at this magnetic field and hence obtain enough data for the type I ELMy H-mode dataset at $B_T$ = 1.7T. An additional deuterium dataset at 1.7MA/1.7T, with D-NBI only, was also obtained. H-NBI operation was at lower NB voltage (70 kV) than with D-NBI (90 – 100 kV). In the hydrogen H-modes at 1.4 MA/1.7T with NBI + ICRH heating, the fraction of heating (as computed by the ICRH deposition code PION [45] including ICRH+NBI synergy [46]) delivered to ions is slightly reduced and the fraction of power delivered to electrons is slightly increased compared to the case with NBI-only heating (as computed by the neutral beam deposition code PENCIL [29]). However, the relative variation is of order 5 – 10 %, depending on the discharge, and thus unlikely to compromise the conclusions drawn on the isotope scaling of energy confinement presented below.

As the input power is increased in experiment after the L-H transition, the plasma first enters the type III ELMy H-mode, at low input power above $P_{L-H}$ and high ELM frequency, $f_{ELM}$. Subsequently, as the auxiliary heating is increased further, the type I ELMy H-mode regime is accessed, at higher β and confinement. The power threshold for the transition from type III to type I ELMs, characterized phenomenologically by $f_{ELM}$ decreasing with power for type III ELMs and $f_{ELM}$ increasing with power for type I ELMs [47], doubles from deuterium to hydrogen, as shown in Figure 15. This is in agreement with findings in JET-C [39] and consistent with the favourable 1/A scaling found for the H-mode threshold in the high density

branch. The variation in $f_{ELM}$ at a given $P_{loss}$, shown in Figure 15, is a consequence of the varying injected gas rates in the hydrogen and deuterium power and gas scan experiments.

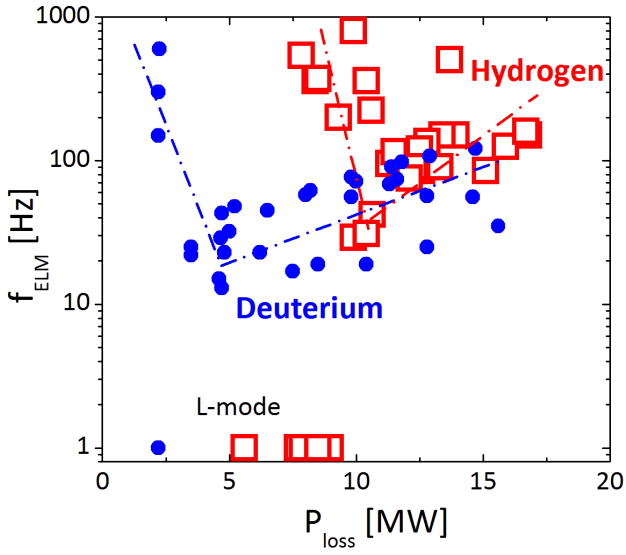


***Figure 15.*** *ELM frequency vs loss power for hydrogen (red open squares) and deuterium (solid blue circles) power and gas scans at 1.4MA/1.7T, low triangularity in JET-ILW, showing doubling of the power threshold for type III to type I ELMs from deuterium to hydrogen plasmas.*

The thermal energy confinement is strongly reduced in hydrogen H-modes, in contradiction of the gyro-Bohm scaling, resulting in a stronger, favourable dependence with isotope mass, $\tau_{E,th} \sim A^{0.4}$, than for the IPB98(y,2) scaling $\tau_{E,th,IPB98(y,2)} = 5.62 \times 10^{-2}\ A^{0.19}\ I_P^{0.93}\ B_T^{0.15}\ R^{1.97}\ \varepsilon^{0.58}\ k_a^{0.78}\ n_e^{0.41}\ P_{abs}^{-0.69}$ (with R the major radius [m], ε the inverse aspect ratio and $k_a$ the plasma elongation) [48]. The hydrogen and deuterium JET-ILW dataset was obtained in plasmas with the same shape, therefore regressions of the $\tau_{E,th}$ data were performed with respect to $I_P$, $B_T$, $P_{abs}$ and A, $n_e$ and gas rate (or $f_{ELM}$). Although isotope mass, plasma density and gas rate (or ELM frequency) are correlated - in addition $n_e$ and Ip are also correlated – the $A^{0.4}$ dependence of $\tau_{E,th}$ on the isotope mass is robust against which combination of this variables is chosen in the regression of the data.

A distinct feature of hydrogen plasmas is the lower plasma density and the fact that the density can be varied with injected gas rate, unlike in the deuterium H-modes, where the density is weakly affected by gas injection [49], [50]. This indicates degraded particle confinement with decreasing isotope mass, as observed in L-mode. In H-modes at the same input power and gas injection rate, a larger pedestal pressure is observed in deuterium than in hydrogen. The difference in pedestal pressure, and therefore total pressure, is primarily due to the larger pedestal density in deuterium than in hydrogen, while the difference in temperature profiles is more modest, as shown in Figure 16 for two type I ELMy H-modes at 1.4MA/1.7T in H and D with $P_{NBI}$ = 10 MW.

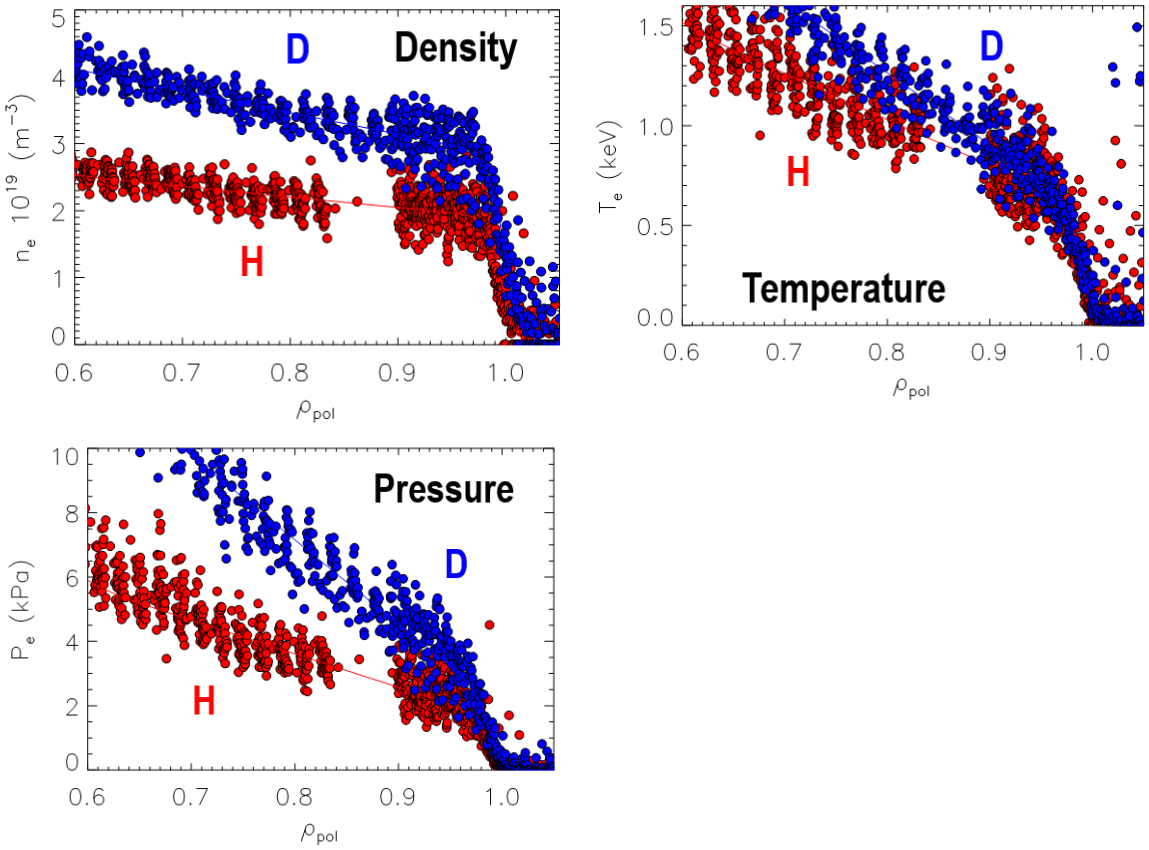


***Figure 16.*** *Composite edge electron kinetic profiles for two type I ELMy H-modes in JET-ILW at the same $I_P/B_T$ = 1.4MA/1.7T, input power $P_{NBI}$ = 10 MW and gas injection rate $\Gamma$ = 3-4 x $10^{21}$ e/s: H (red, #91554) and D (blue, #84796). $T_i = T_e$ both in H and in D, within the uncertainties in the ion temperature measurements and the line averaged $Z_{eff}$ ~ 1.4 with both isotopes. The profiles were measured HRTS and are ELM-averaged over steady time intervals of the discharges (6.2 – 8.2 s for the H discharge and 5.3 – 6.45 s for the D discharge). The solid lines are hyperbolic tangent fits to the data.*

H-modes in hydrogen and deuterium at the same thermal stored energy, $W_{th}$, do not have matched density and temperature profiles: in hydrogen the lower density is compensated by higher temperature. This contrasts JT-60U experiments, where the density and temperature profiles were matched for the two species when $W_{th}$ was matched by raising the H-NBI heating, as discussed above. This difference suggests different particle transport in the two tokamaks and warrants further investigations in order to enable extrapolation of present-day experimental results to ITER and beyond.

Across the isotope dataset obtained in JET-ILW, the electron pedestal pressure, $p_{e,PED}$, is larger in deuterium than in hydrogen type I ELMy H-modes, as shown in Figure 17 for the 1.4MA/1.7T data. Similarly, also the ion pedestal pressure is larger in deuterium than in hydrogen, as $T_{i,PED}$ ~ $T_{e,PED}$ consistently throughout the dataset for both ion species and $Z_{eff}$ (primarily determined by the Be intrinsic impurity) varies between 1.1 and 1.4 in deuterium and between 1.1 and 1.7 in hydrogen, depending on $I_P/B_T$ and input power. Interestingly, hydrogen and deuterium pedestals are found to react differently to variations in gas rate and

input power: whereas hydrogen pedestals evolve along the same isobar, exchanging temperature for density as the gas rate is increased and/or the input power is reduced, in deuterium it is primarily $T_{e,PED}$ to be reduced with increasing gas rate, while $n_{e,PED}$ is little affected by varying levels of injected gas. An increase in input power in deuterium – at a given gas rate – leads to an increase in $T_{e,PED}$ and a decrease in $n_{e,PED}$ (via the increase in $f_{ELM}$ for type I ELMs). Thus, especially at the lowest gas rate in the scan (see Figure 17) the pedestal pressure of deuterium plasmas increases with power, see e.g. [49].

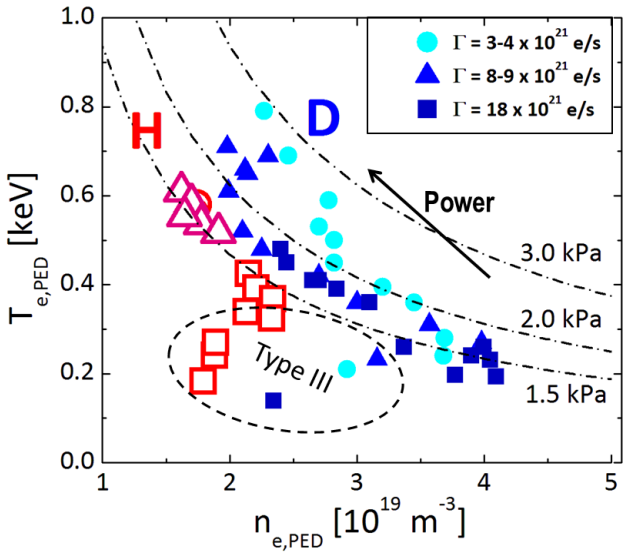


***Figure 17.*** *$T_{e,PED}$ – $n_{e,PED}$ diagram for H and D power and gas scans at 1.4MA/1.7T, low plasma triangularity in JET-ILW.*

As discussed for the L-mode dataset in Section 2, also the H-modes of this study have relatively high collisionality, leading to strong electron-ion coupling, and the core $T_i$ profile data have large uncertainties (~ 20%). Therefore, in these conditions, a meaningful species-resolved transport analysis is unfortunately not possible. Across the entire type I ELMy H-mode dataset, both in hydrogen and in deuterium, the transport analysis has been carried out based on the electron kinetic profiles. As for the L-mode discharges, also in the H-mode dataset the sawtooth inversion radius is at $\rho_{tor}$ = 0.22 – 0.26, depending on the individual discharge, where $q_\psi$ ~1. In the transport region, the inverse normalized temperature gradient length is measured for electrons, $R/L_{Te}$ ~~($\cong R/L_{Ti}$)~~, for both isotope species. Also in type I ELMy H-modes the ions and/or the electrons are stiff. In this sense, there is no difference between L-mode and H-mode core behaviour. Figure 18 shows the one fluid, effective heat diffusivity, $\chi_{eff}$, at mid radius ($\rho_{tor}$ = 0.5) for the hydrogen and deuterium type I ELMy H-mode dataset. There is little overlap in $\chi_{eff}$ in hydrogen and deuterium H-modes, due to the large difference in auxiliary heating required to access type I ELMy H-mode in the two species and due to the plasma density being systematically lower in hydrogen than in deuterium.

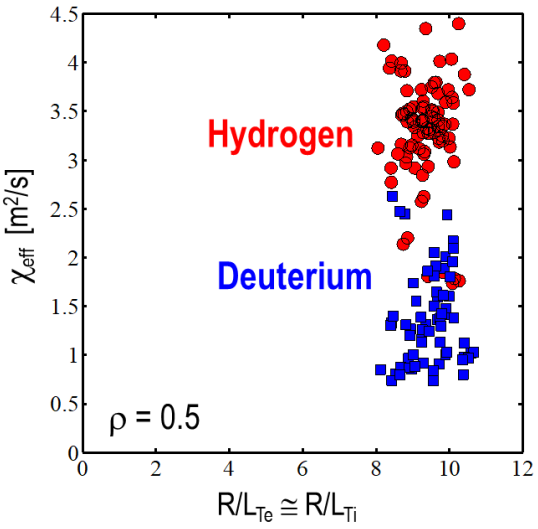


***Figure 18.*** *One-fluid effective heat diffusivity, $\chi_{eff}$, vs $R/L_{Te} \cong R/L_{Ti}$ at $\rho_{tor}$ = 0.5 for the JET-ILW type I ELMy H-mode isotope dataset: hydrogen (red) at 1.0MA/1.0T and 1.4MA/1.7T; deuterium (blue) at 1.0MA/1.0T, 1.4MA/1.7T and 1.7MA/1.7T.*

In contrast to JT-60U, the combination of larger pedestal pressure in deuterium and constant $R/L_T$ for both plasma species suggests for JET-ILW type I ELMy H-modes that the favourable isotope effect on $\tau_{E,th}$ propagates from the pedestal through the plasma core via constant critical temperature gradient.

Possible contributing factors to the isotope effect observed in the pedestal region could be due to the isotope mass dependence in the edge bootstrap current, which plays a key role in the H-mode edge stability, and/or in the micro-instabilities that drive the residual edge transport levels inter-ELMs. Both these aspects will be addressed in future studies.

## 5. Summary and Conclusions

Recent isotope experiments in hydrogen and deuterium in JET-ILW have yielded a wealth of new results concerning the isotope effects on L-mode and H-mode confinement and transport and on the L-H power threshold.

In L-mode, $\tau_{E,th}$ is found to scale weakly with isotope mass, $\tau_{E,th} \sim A^{0.15}$, in contradiction of the gyro-Bohm (and the Bohm) scaling, and in analogy with findings from most tokamak L-mode experiments, as expressed by the ITER-97L scaling, $\tau_{E,th} \sim A^{0.2}$. A negligible isotope effect on heat transport is found in the plasma core and a strong, positive isotope effect is found at the plasma edge, both inside and outside the LCFS, on energy and particle transport. Larger edge density fluctuations in hydrogen than in deuterium at the same input power corroborate the larger particle transport coefficient obtained by interpretative EDGE2D/EIRENE modelling of upstream edge density profiles. The favourable 1/A scaling of $P_{L-H}$ is confirmed in the high density branch in ICRH heated plasmas, whereas a stronger isotope dependence is observed in the low density branch, which is suggestive of L-mode edge turbulence of different nature in the two density branches of $P_{L-H}$. It is suggested that the isotope effect on $P_{L-H}$ in the high density branch, $P_{L-H} \sim 1/A$, may be linked to the

favourable isotope effect on transport at the L-mode edge. In turn, the isotope effect on $P_{L-H}$ is likely to propagate to the isotope effect measured on the power threshold for type III to type I ELMs, $P_{typeIII-typeI} \sim 1/A$, and to the strong, favourable isotope effect on thermal energy confinement time measured in type I ELMy H-modes, $\tau_{E,th} \sim A^{0.4}$. This is in contradiction of the gyro-Bohm scaling, which would predict $\tau_{E,th} \sim A^{-0.5}$. On the other hand, in deuterium plasmas the dimensionless energy confinement time follows the gyro-Bohm scaling, $\Omega\tau_E \sim \rho^{*-3}$ [51], in agreement with experimental results from several other tokamaks, including JET-C, see e.g. [2] and references therein (where $\Omega = eB/A$ is the cyclotron frequency, $\tau_E \sim a^2/\chi$ and $\chi/\chi_B \sim \rho^*$, with $\chi_B = T/ZeB$ the Bohm diffusivity [2]). As previously shown in JET-C, and in contrast to JT-60U findings, in JET-ILW the isotope effect is found at the pedestal and it propagates through the plasma core via constant critical temperature gradient in conditions where ions and electrons are strongly coupled and/or the ion heat transport is stiff. On the other hand, it is possible that in plasmas with weak ion-electron coupling the ion transport could be different and, consequently, an additional isotope effect on core ion transport may arise in such conditions.

Overall, a favourable isotope effect on confinement and $P_{L-H}$ is observed in tokamak experiments, which projects favourably to a future reactor that will operate in deuterium-tritium mixtures. The isotope dependence observed in experiment is in contradiction of the gyro-Bohm scaling, both in the L-mode and in the H-mode regime, while gyro-Bohm scaling of the thermal energy confinement is consistently confirmed in deuterium in H-mode experiments from many tokamaks. This discrepancy still presents a main challenge to the understanding of plasma turbulent transport and, despite many recent advances in theory, needs to be investigated further with extensive isotope studies across multiple tokamaks.

Indeed, recent numerical studies of an ITER modelling scenario, with non-linear gyrokinetic simulations, have shown that the core plasma micro-turbulence can depend on the isotope mass via multi-scale non-linear effects involving zonal flows, electromagnetic effects and *ExB* shear [26]. The local, gyro-Bohm scaling of plasma micro-turbulence is thus counteracted by the above effects, leading to isotope effects on heat transport on longer scale lengths [26], [52]. On the other hand, these theoretical analyses are highly relevant to the interpretation of isotope effects observed in high beta plasmas, such as the hot ion H-modes of TFTR [53] or future hybrid deuterium-tritium plasmas in JET, where observation of these effects likely requires that ions are thermally decoupled from the electrons, unlike the JET experiments reported in this paper. Further theoretical work is required to understand the strong isotope effect measured at the pedestal of JET-ILW H-modes, or the isotope effect found in Ohmic and low beta JET-ILW L-modes.

Different results and interpretations of the isotope effects obtained across tokamak experiments, e.g. the contrasting results in H-mode from JT-60U and JET-C and JET-ILW discussed in Section 4, may be related to a variety of factors, such as different plasma heating methods, the role of $T_i/T_e$ on ion-scale core turbulence, the impact of *ExB* flow shear stabilization in the plasma core, high beta stabilization of ion-scale core turbulence, the impact of impurities. Such studies will be undertaken in JET in the upcoming isotope campaigns leading to deuterium-tritium experiments with the ITER-like wall, in support of ITER research.

**Acknowledgements**
Useful discussions with Dr M Mantsinen are gratefully acknowledged.

This work was carried out within the framework of the EUROfusion Consortium and received funding from the Euratom research and training programme 2014-2018 under grant agreement No 633053 and from the RCUK Energy Programme grant No EP/P012450/1. The views and opinions expressed herein do not necessarily reflect those of the European Commission. To obtain further information on the data and models underlying this paper please contact PublicationsManager@ukaea.uk.

**References**

[1] Hinton FL and Hazeltine RD 1976 *Rev. Mod. Phys.* ***48*** *239.*
[2] Luce TC, Petty CC and Cordey JG 2008 *Plasma Phys. Control. Fusion* ***50*** *043001.*
[3] Petty CC et al., 1995 *Phys. Rev. Lett.* ***74*** *1763.*
[4] Christiansen JP et al., 1993 *Nucl. Fusion* ***33*** *863.*
[5] Burrell KH et al., 1992 *Plasma Phys. Control. Fusion* ***34*** *1859.*
[6] Connor JW and Wilson HR 2000 *Plasma Phys. Control. Fusion* ***42*** *R1.*
[7] Maggi CF et al., 2007 *Nucl. Fusion* ***47*** *535.*
[8] Saarelma S et al., *"Integrated modelling of H-mode pedestal and confinement in JET-ILW", 2017 Plasma Phys. Control. Fusion in press* https://doi.org/10.1088/1361-6587/aa8d45
[9] ASDEX Team, 1989 *Nucl. Fusion* ***29*** *1959.*
[10] Bessenrodt-Weberpals M et al., 1993 *Nucl. Fusion* ***33*** *1205.*
[11] Schissel DP et al., 1989 *Nucl. Fusion* ***29*** *185.*
[12] Tibone F et al., 1993 *Nucl. Fusion* ***33*** *1319.*
[13] Barnes CW et al., 1996 *Phys. Plasmas* ***3*** *4521.*
[14] Cordey JG et al., 1999 *Nucl. Fusion* ***39*** *301.*
[15] Urano H et al., 2008 *Nucl. Fusion* ***48*** *045008.*
[16] Urano H et al., 2012 *Phys. Rev. Lett.* ***109*** *125001.*
[17] Urano H et al., 2013 *Nucl. Fusion* ***53*** *083003.*
[18] Schneider P et al. 2017 *Nucl. Fusion* ***57*** *066003.*
[19] Laggner F et al., 2017 *Phys. Plasmas* ***24*** *56105.*
[20] Niskala P et al., 2017 *Plasma Phys. Control. Fusion* ***59*** *044010.*
[21] Gurchenko AD et al., 2016 *Plasma Phys. Control. Fusion* ***58*** *044002.*
[22] Scott SD et al., 1995 *Phys Plasmas* ***2*** *2299.*
[23] Jacquinot J and JET TEAM 1999 *Nucl. Fusion* ***38*** *1263.*
[24] Scott SD et al., 1996 *Proc. 16th Fusion Energy Conference, Montreal,* ***1****, 573.*
[25] Bustos A et al., 2015 *Phys. Plasmas* ***22*** *012305.*
[26] Garcia J et al., 2017 *Nucl. Fusion* ***57*** *014007.*
[27] Kaye SM et al. 1997 *Nucl. Fusion* ***37*** *1303.*
[28] Delabie E et al., 2017 "*Preliminary interpretation of the isotope effect on energy confinement in Ohmic discharges in JET-ILW", 44th EPS Conference on Plasma Physics, Belfast, June 2017, P4.159.*
[29] Challis CC et al., 1989 *Nucl Fusion* ***29*** *563.*
[30] Goldston RJ et al, 1981 *J.Comp.Phys* ***43*** *61.*
[31] R Simonini et al., 1994 *Contrib. Plasma Phys.* ***34*** *368.*
[32] D Reiter, 1992 *J. Nucl. Mater.* ***196-198*** *80.*

[33] Day C, “Basics and applications of cryopumps”, http://cds.cern.ch/record/1047069/files/p241.pdf
[34] Hillesheim JC et al., 2016 *Phys. Rev. Lett.* ***116*** *065002.*
[35] Y Martin et al., 2008 *J. Phys. Conf. Ser.* ***123*** *012033.*
[36] JFT-2M Group, 1991 *Proc. 3rd H-mode Workshop, Vol. 1 141.*
[37] Gohil P et al., 2010 Nucl. Fusion **50** 064011.
[38] Ryter F et al., 2013 *Nucl. Fusion* ***53*** *113003.*
[39] Righi E et al., 1999 *Nucl. Fusion* ***39*** *309.*
[40] Hillesheim J et al., 2017 *“L-H transition studies in hydrogen and mixed ion species plasmas in JET”, 44th EPS Conference on Plasma Physics, Belfast, June 2017, P5.162.*
[41] Delabie E et al., 2015 “*Recent L-H threshold results in hydrogen plasmas in JET-ILW”, 57th Annual Meeting of the APS Division of Plasma Physics, Savannah, USA, November 2015.*
[42] Ryter F et al., 2014 *Nucl. Fusion* ***54*** *083003.*
[43] King DB et al., 2017 *“Mixed Hydrogen-Deuterium plasmas on JET-ILW: H-mode confinement and isotope mixture control”, 44th EPS Conference on Plasma Physics, Belfast, June 2017, O3.112.*
[44] Bhatnagar VP et al., 1999 *Nucl. Fusion* ***39*** *353.*
[45] Eriksson LG et al., T. 1993 *Nucl. Fusion* ***33*** *1037.*
[46] Mantsinen MJ et al., 1999 *Plasma Phys. Control. Fusion* ***41*** *843.*
[47] Zohm H et al., 1996 *Plasma Phys. Contro.l Fusion* ***38*** *105.*
[48] ITER Physics Basis 1999 *Nucl. Fusion* ***39*** *2175.*
[49] Maggi CF et al., 2015 *Nucl. Fusion* ***55*** *113031.*
[50] Urano H et al., 2016 *“Characterization of electron density based on operational parameters in JET H-mode plasmas with C and ILW”, 43rd EPS Conference on Plasma Physics, Louven, June 2016, O4.121.*
[51] Frassinetti L et al., 2017 *Plasma Phys. Control. Fusion* ***59*** *014014.*
[52] Hennequin P et al., 2015 *“Comprehensive experimental study of plasma turbulence structure and its scaling with $\rho^*$”, 42nd EPS Conference on Plasma Physics, Lisbon, June 2015, p I1.102.*
[53] Ernst DR et al., 1998 *Phys. Rev. Lett.* ***81*** *2454.*